

Supplementary Materials for

Biomimetic potassium-selective nanopores

Elif Turker Acar*, Steven F. Buchsbaum*, Cody Combs, Francesco Fornasiero*, Zuzanna S. Siwy*

*Corresponding author. Email: zsiwy@uci.edu (Z.S.S.); elifacar@istanbul.edu.tr (E.T.A.);
buchsbaum1@llnl.gov (S.F.B.); fornasiero1@llnl.gov (F.F.)

Published 8 February 2019, *Sci. Adv.* **5**, eaav2568 (2019)
DOI: 10.1126/sciadv.aav2568

This PDF file includes:

Fig. S1. Examples of I - V curves for the nanopores shown in Fig. 1 before crown ether attachment.

Fig. S2. Selectivity of nanopores shown in Fig. 1 toward potassium ions at -1 V.

Fig. S3. Ion selectivity at 1 V of a nanopore modified with crown ether from one side only.

Fig. S4. Ion current through a 1-nm-diameter nanopore modified with DNA from one side.

Fig. S5. Ion currents through a nanopore shown in Fig. 1C as a function of KCl and NaCl concentrations.

Fig. S6. Scheme of a modeling system used to predict local ionic concentrations and electric potential in a nanopore.

Fig. S7. Results of numerical modeling of ionic concentrations and electric potential in a nanopore shown in fig. S6.

Fig. S8. I - V curves for the nanopore shown in Fig. 4.

Table S1. Pore opening diameters calculated according to Eq. 1 for all nanopores considered in the manuscript.

1. Current-voltage curves of nanopores before and after TESMPA modification.

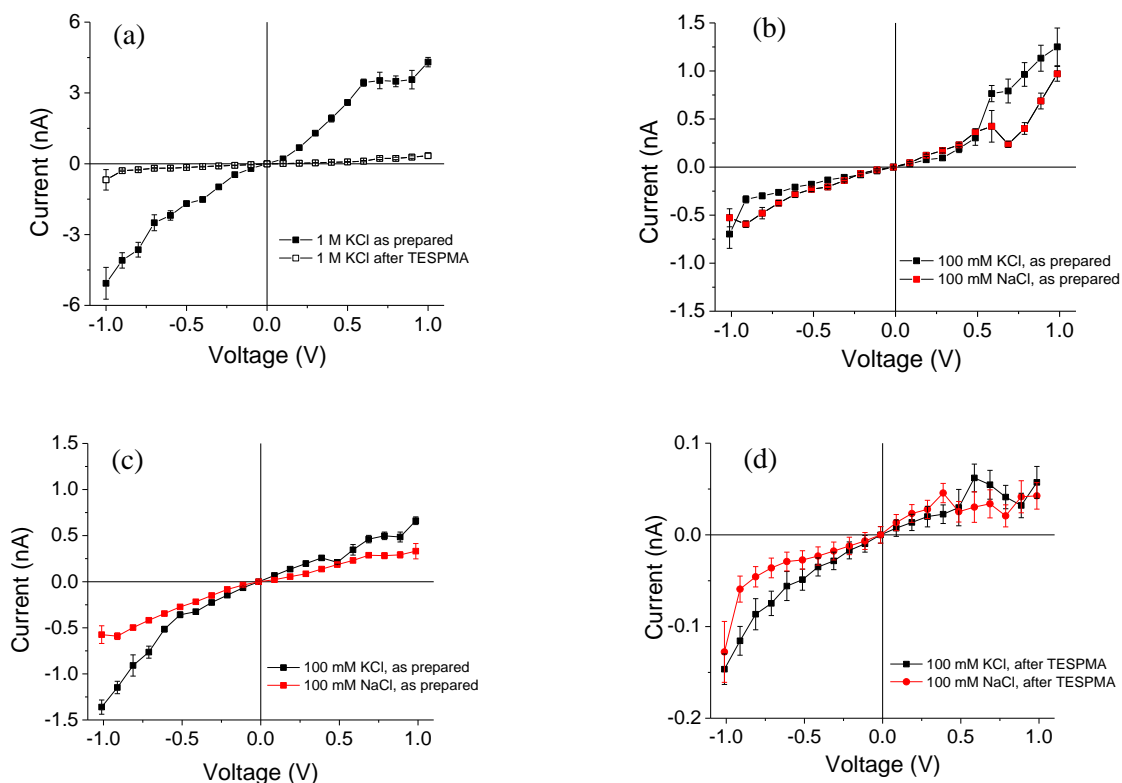


Fig. S1. Examples of I - V curves for the nanopores shown in Fig. 1 before crown ether attachment. (a) Current-voltage curves of the as prepared nanopore shown in Fig. 1b before and after modification with TESMPA. The effective opening diameter calculated with eq. (1) from recordings in 1 M KCl was 4 nm before TESMPA, and 1 nm after the modification. (b) Current-voltage curves of the as prepared nanopore of Fig. 1b in 100 mM KCl and 100 mM NaCl. (c,d) Current-voltage curves in 100 mM KCl and NaCl before and after TESMPA modification for the pore shown in Fig. 1c. This pore was originally 6 nm in diameter, and 0.6 nm after TESMPA.

2. Potassium selectivity of nanopores at -1V (see Fig. 1 in the main manuscript).

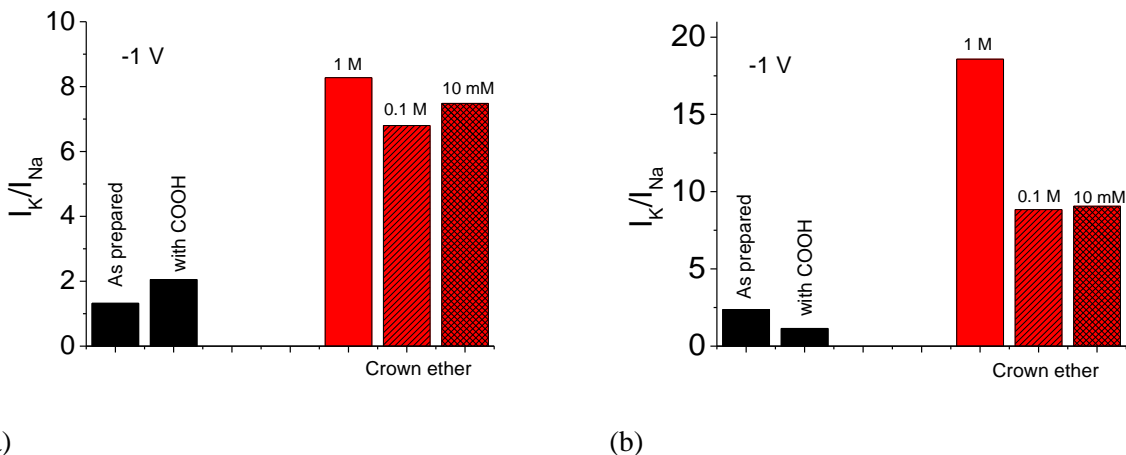


Fig. S2. Selectivity of nanopores shown in Fig. 1 toward potassium ions at -1 V. (a) A nanopore modified only with crown ether (Fig. 1b); (b) A nanopore modified with crown ether and DNA (Fig. 1c). Selectivity of the pores before modification with crown ether was calculated based on recordings in 100 mM KCl and NaCl.

3. Data for a nanopore subjected to chemical modification with crown ether from one side only.

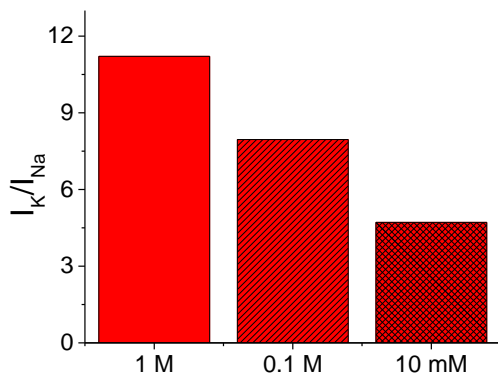


Fig. S3. Ion selectivity at 1 V of a nanopore modified with crown ether from one side only. After carboxylation with TESMPA, this pore had an opening diameter of 1.4 nm.

4. Data for a nanopore subjected to chemical modification with ssDNA from one side only.

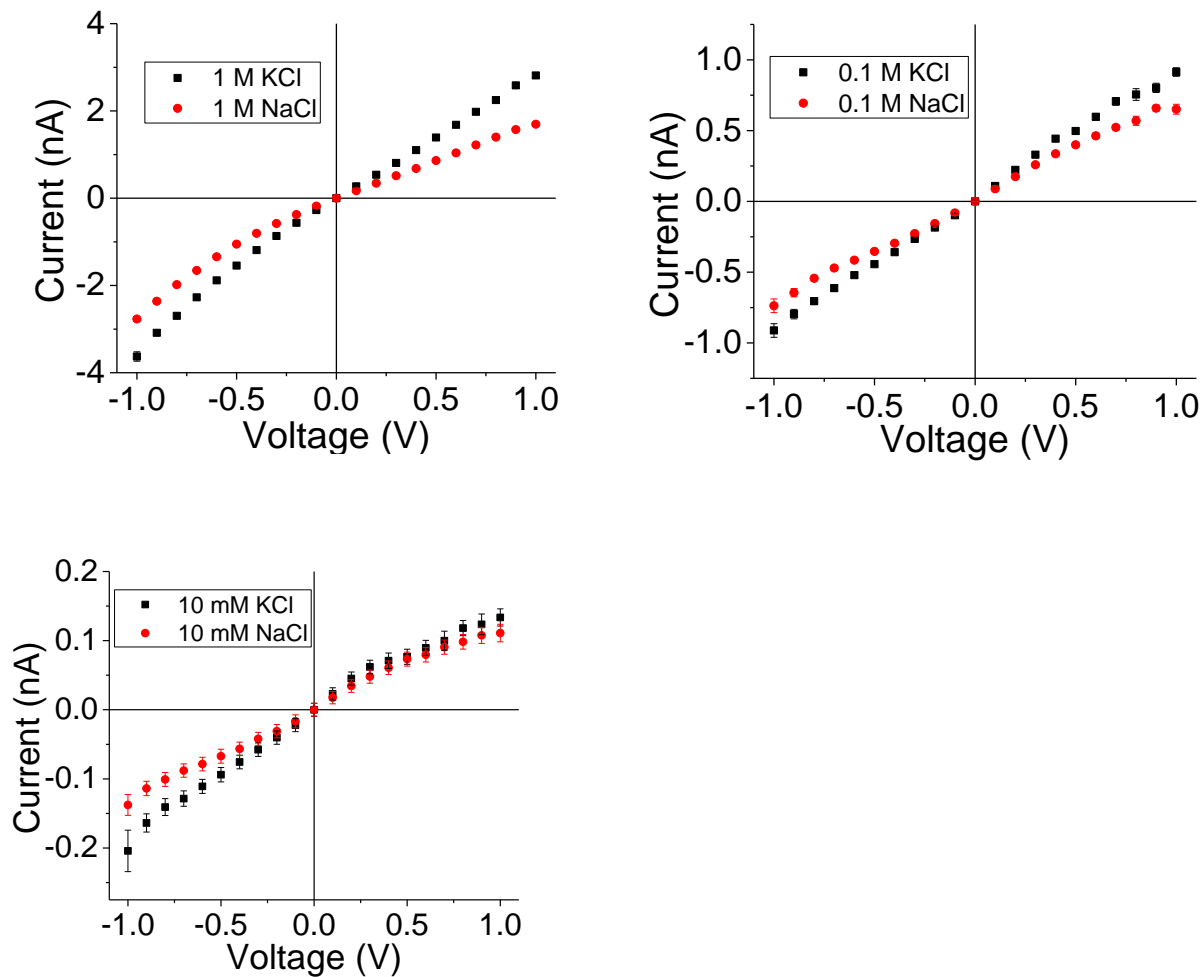


Fig. S4. Ion current through a 1-nm-diameter nanopore modified with DNA from one side.

Recordings in 1 M, 100 mM and 10 mM of KCl and NaCl are shown.

5. Ion currents of a DNA/crown ether modified nanopore in KCl and NaCl.

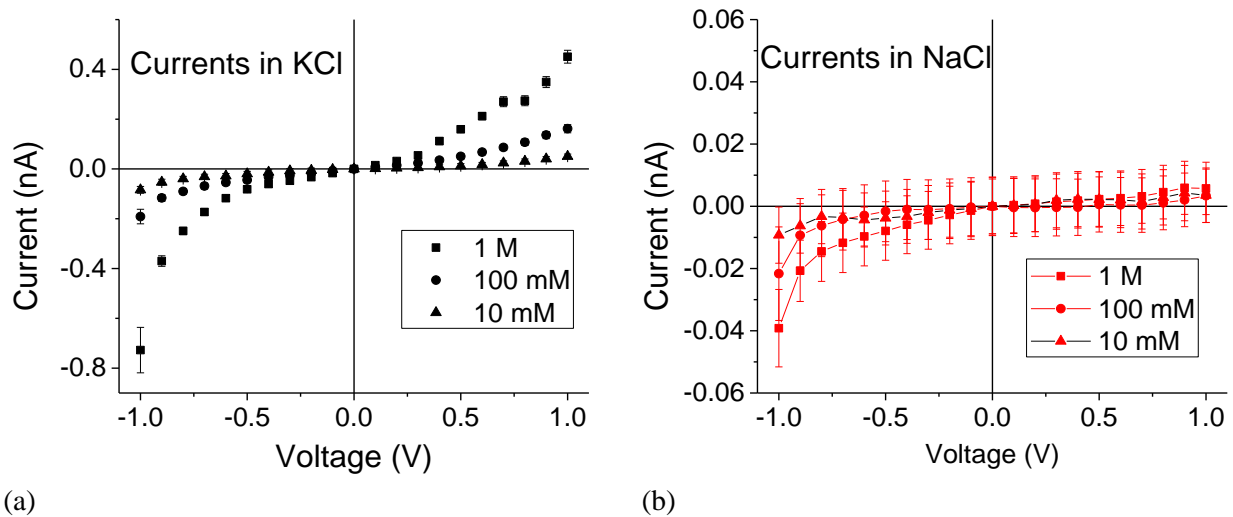


Fig. S5. Ion currents through a nanopore shown in Fig. 1C as a function of KCl and NaCl concentrations. The nanopore was modified with crown ether and DNA.

6. Continuum modeling of ionic concentrations and electric potential inside a nanopore.

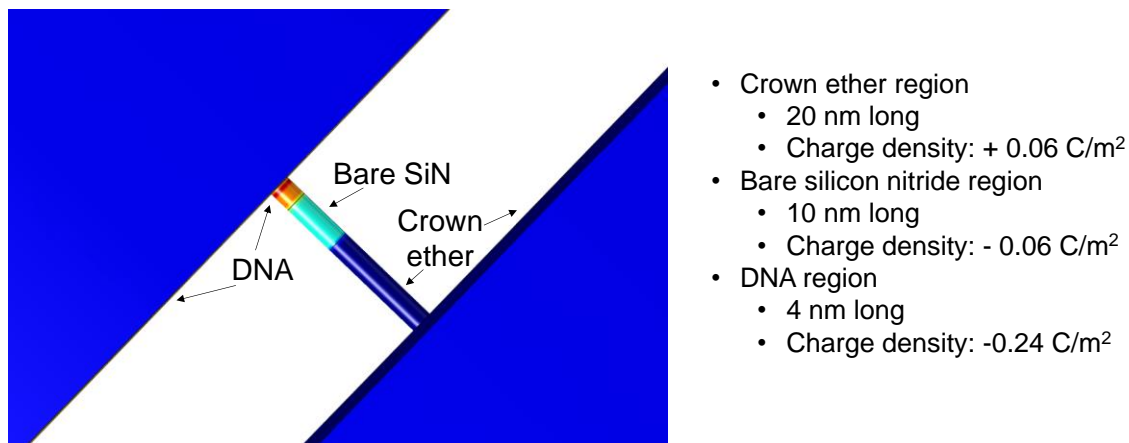


Fig. S6. Scheme of a modeling system used to predict local ionic concentrations and electric potential in a nanopore. The nanopore considered was 30 nm in length and 3 nm in diameter; the larger opening compared to the nanopores probed experimentally was chosen to be able to apply a continuum approach based on the Poisson-Nernst-Planck (PNP) equations. PNP equations were solved numerically using Comsol Multiphysics 5.3 package. The presence of crown ether was considered as a positively charged region. Lengths and charge densities of the zones modified with crown ether and DNA as well as of the zone with bare silicon nitride are given in the legend.

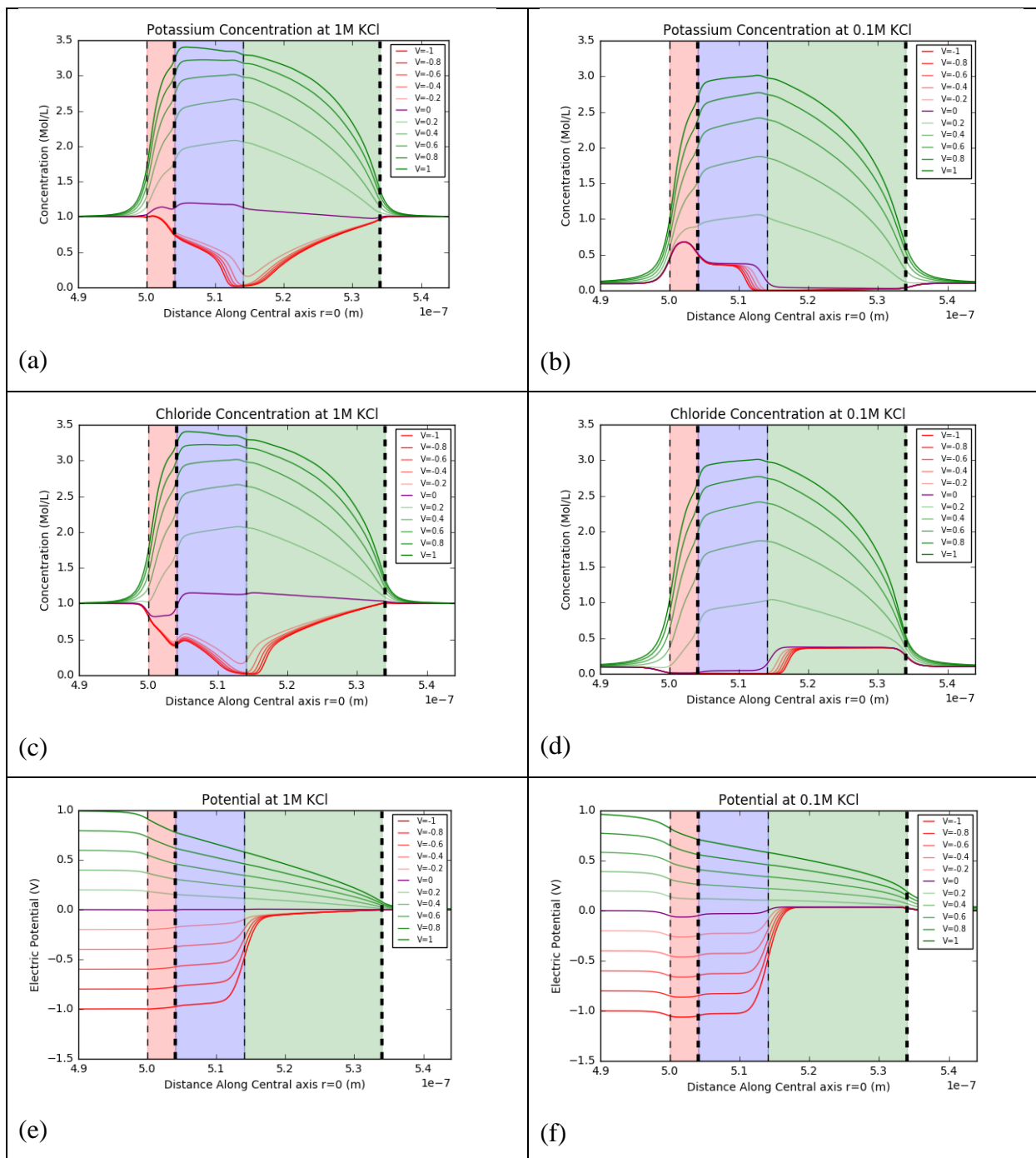


Fig. S7. Results of numerical modeling of ionic concentrations and electric potential in a nanopore shown in fig. S6. Poisson-Nernst-Planck equations were solved numerically. The region with DNA is marked in pink, the purple region corresponds to bare silicon nitride, and the green region to the part of the pore modified with crown ether. (a-d) Profiles of potassium ions concentrations (a,b) and chloride ions concentrations (c,d) in 1 M KCl and 0.1 M KCl. (e,f)

Distribution of electric potential along the pore axis in 1 M KCl and 0.1 M KCl. Ionic concentrations shown are the values on the pore axis. Note that only electrostatic interactions are considered; specific interactions of potassium ions with crown ether were not taken into account in this model.

7. Current-voltage curves recorded for a 1 nm nanopore modified with ssDNA and crown ether in mixtures of KCl and NaCl.

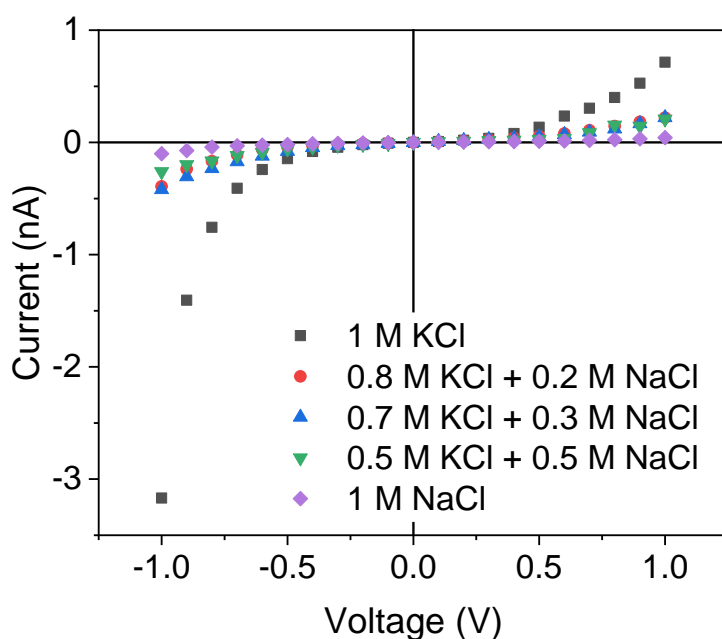


Fig. S8. *I-V* curves for the nanopore shown in Fig. 4. Recordings were performed in mixtures of KCl and NaCl, as indicated in the legend, as well as 1 M KCl and 1 M NaCl.

8. Modeling of facilitated transport through crown ether modified pores.

The model consists of a cylindrical pore with radius R_p and length L_p which has a constant radial thickness of crown ether modification attached to the inner wall, defined as R_{mod} . For $R_p < R_{mod}$ the entire pore is assumed to be filled with crown ethers while for $R_p > R_{mod}$ the crown ether

filled region corresponds to $(R_p - R_{mod}) < r < R_p$. Current through the modified region is modeled as facilitated transport governed by binding and unbinding of the ions and crown ether molecules. The binding and unbinding events are governed by the rate constants k_{on} and k_{off} that depend exponentially on the applied voltage, V , as

$$k_{i,j} = k_{i,j0} e^{-\frac{d_{ce}eV}{L_p k_B T}}$$

where $i = on, off, j = ion\ type$, $\frac{d_{ce}}{L_p}$ corresponds to the fractional potential drop an ion experiences as it approaches and binds to a crown ether, $k_{i,j0}$ are the binding rate when no potential is applied, e is the unit charge, k_B is the Boltzmann constant, and T is the temperature. For simplicity, only transport through a single layer of crown ether molecules is considered. This allows to write the total time an ion takes to pass through the pore, τ , as

$$\tau_j = \frac{1}{k_{on,j}C} + \frac{1}{k_{off,j}}$$

where C is the ion concentration. The charge density in the crown ether modified region of the pore is calculated assuming there is one charged ion per crown ether volume, ν_{ce} , and that the percentage of bound ion-crown ether complexes is given by the equation

$$b_{ce,j} = \frac{K_j C_j}{1 + K_K C_K + K_{Na} C_{Na}}$$

with K defined as the ratio $\frac{k_{on}}{k_{off}}$. The current through this part of the pore can then be expressed

as

$$I_{ce} = \sum_j \pi [R_p^2 - (R_p - R_{mod})^2] * l_{ce} (\tau_{F,j}^{-1} - \tau_{R,j}^{-1}) * \frac{e}{\nu_{ce}} * b_{ce,j}$$

where l_{ce} represents the width of a crown ether molecule and $\tau_F = \tau(V)$ and $\tau_R = \tau(-V)$ are the translocation times for ions moving with or against the applied potential, respectively. When $R_p > R_{mod}$, we assumed bulk transport behavior in the pore volume not filled by crown ethers, which is defined by $0 < r < (R_p - R_{mod})$. This current is modeled as

$$I_l = \sum_j \frac{\kappa_j \pi R_{in}^2 V}{L_p}$$

with κ representing the bulk conductivity of the electrolyte solution. The total current through the pore can then be written by summing the two contributions over the entire pore radius, given by $I = I_{ce} + I_l$. Finally, the ion selectivity is defined as $\frac{I_K}{I_{Na}}$ where I_K is the current in KCl and I_{Na} is the current in NaCl solution. In the case of mixed salt solutions, the ion selectivity is defined as $\frac{I_{Mixture}}{I_{Na}}$ where $I_{Mixture}$ is the current in the mixed salt solution.

9. Fitting to experimental data

Fitting was done in Mathematica using the NonlinearModelFit function with the minimization method set to NMinimize. Initial parameter guesses were $3.7 \times 10^6 \text{ s}^{-1}$, $4.3 \times 10^8 \text{ s}^{-1}\text{M}^{-1}$, $3.4 \times 10^7 \text{ s}^{-1}$, $2.2 \times 10^8 \text{ s}^{-1}\text{M}^{-1}$, and 3 nm for $k_{off0,K}$, $k_{on0,K}$, $k_{off0,Na}$, $k_{on0,Na}$, and d_{ce} respectively, with the binding rate values taken from the literature on bulk solutions. k_{off} and k_{on} were bounded between 5×10^5 and $1 \times 10^{10} \text{ s}^{-1}$ (or $\text{s}^{-1}\text{M}^{-1}$), while d_{ce} was bounded between 0.1 and 5 nm. The dataset, $\{x_i\}$, was weighted using a factor of $\{1/x_i\}$ in order to account for the large possible range of values.

Table S1. Pore opening diameters calculated according to Eq. 1 for all nanopores considered in the manuscript.

| | Pore Diameter | |
|-----------------|--------------------------------|-------------------------------|
| | Before TESMPA modification, nm | After TESPMA modification, nm |
| P17 (Crown) | 4.0 | 1 |
| P42 (Crown) | 8.7 | 1.4 |
| P4 (Crown) | 4.3 | 1.7 |
| P54 (Crown+DNA) | 7.2 | 0.3 |
| P14 (Crown+DNA) | 4.7 | 0.6 |
| P8 (Crown+DNA) | 5.0 | 1.1 |
| P11(Crown+DNA) | 7.0 | 2.0 |
| P49 (Crown+DNA) | 23 | 3.2 |
| P21 (Crown+DNA) | 17 | 6.7 |
| P3 (Crown+DNA) | 6.0 | 1.0 |